

Chemical freeze-out in heavy ion collisions at large baryon densities

Stefan Floerchinger¹ and Christof Wetterich²

¹*Physics Department, Theory Unit, CERN, CH-1211 Genève 23, Switzerland*

²*Institut für Theoretische Physik, Universität Heidelberg, Philosophenweg 16, D-69120 Heidelberg*

We argue that the chemical freeze-out in heavy ion collisions at high baryon density is not associated to a phase transition or rapid crossover. We employ the linear nucleon-meson model with parameters fixed by the zero-temperature properties of nuclear matter close to the liquid-gas quantum phase transition. For the parameter region of interest this yields a reliable picture of the thermodynamic and chiral properties at non-zero temperature. The chemical freeze-out observed in low-energy experiments occurs when baryon densities fall below a critical value of about 15 percent of nuclear density. This region in the phase diagram is far away from any phase transition or rapid crossover.

Relativistic heavy ion collisions are a promising way to investigate the properties of fundamental quantum field theory – more specific QCD – at nonzero temperature and density. However, in contrast to most condensed matter systems the produced matter has only a short live time during which it expands and cools quickly. It is a big challenge to determine the properties of the produced matter. Basically all information has to be reconstructed from the final state, i. e. from the momenta and chemical composition of the detected particles.

Important observables are the yields of different particle species. To surprisingly good approximation they can be described by the so called statistical model which assumes a thermal distribution of a non-interacting hadron resonance gas [1–3]. The most prominent observables extracted from the thermal fits are the temperature and baryon chemical potential associated with the chemical freeze-out.

It has been advocated that the chemical freeze-out temperature coincides with the temperature of the QCD phase transition for low baryon density [4]. The basic argument states that the rates of particle number changes in the hadronic phase are too small to maintain chemical equilibrium. This holds whenever scattering processes involving only a few particles dominate. Chemical freeze-out therefore occurs for particle number densities that are just high enough that multi-particle scattering or collective effects dominate. For low baryon number that is possible only for temperatures very close to a phase transition or crossover. The difference between the critical temperature and the freeze-out temperature has been estimated to be less than 5 MeV. The measured freeze-out temperature at RHIC at heavy ion collisions with $\sqrt{s_{NN}} = 200$ GeV of 164 ± 6 MeV [3] agrees actually rather well with the critical temperature of the crossover in lattice simulations of $T_c \approx (157 \pm 10)$ MeV [5] and $T_c \approx (154 \pm 9)$ MeV [6].

The agreement between the critical temperature of a phase transition or crossover and the observed chemical freeze-out temperature is expected to hold for low values of the chemical potential μ in the QCD phase diagram. Naturally, the question arises whether a similar argument can be extended to higher values of μ or larger baryon density. Interesting ideas for this issue have been pro-

posed recently [7]. We ask: does the curve of measured freeze-out temperatures reflect a phase transition line or rapid crossover in the whole μ - T -plane?

In this letter we argue that this is not the case. The observed freeze-out temperatures T_{ch} for the largest values of μ lie actually in a region where a simple modeling by baryons and mesons becomes possible. While a rapid change of the particle density with temperature continues to play a crucial role for the determination of T_{ch} , this actually happens in a region that is substantially away from any transition or crossover. We illustrate the situation in Fig. 1 where we indicate the observed points in the μ - T -plane and the region of validity of a simple baryon-meson model. We also demonstrate in Fig. 2 the change of particle density with temperature for fixed value of μ . The dot in this figure indicates the measured value of T_{ch} for $\mu = 760$ MeV. A similar figure 3 for the chiral order parameter σ_0 as a function of T shows that no particular distinct feature such as a (chiral) phase transition or crossover is visible in this range. The deviations of σ_0 from the vacuum value are small in the whole range of the black solid curve in Fig. 1.

For a discussion of the phase diagram and the thermodynamic and chiral properties within the region indicated in Fig. 1 the linear nucleon-meson model is a reasonable approximation. It uses as degrees of freedom the proton and neutron, a neutral vector meson ω_μ as well as the pions and the collective σ -meson. (We ignore isospin violation and electromagnetism for simplicity.) Chiral symmetry is implemented explicitly. Integrating out the σ -degree of freedom yields an effective non-linear σ -model coupled to nucleons and the vector meson. For this latter model the chiral perturbation theory has been used extensively [8]. On the other hand, within a quadratic approximation to the effective potential of the field σ , and if only the dominant nucleon fluctuations are included for the computation of the chiral order parameter and the baryon density, one recovers the gap equations of the Walecka model [9]. Parameters of the effective potential at zero temperature and the chemical potential μ_c corresponding to the gas-liquid phase transition in nuclear matter can be determined from observation. In this parameter region the model can be mapped directly to the nuclear droplet model.

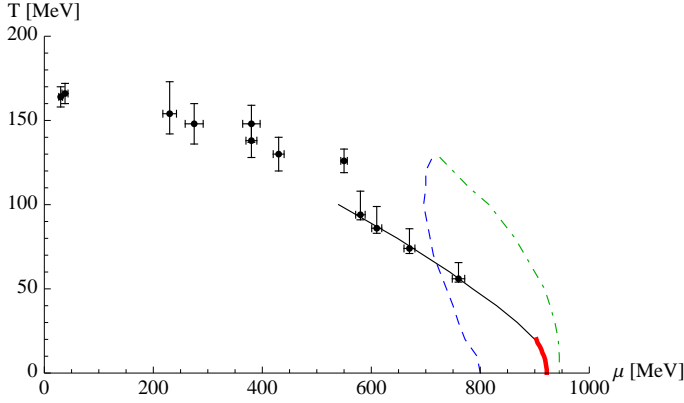


FIG. 1: Curve of constant baryon number $n_{\text{Baryons}} = 0.15 n_{\text{nuclear}}$ in the Meson-Baryon model (solid black line). The points with error-bars mark the chemical freeze-out as obtained from the fits to experimentally measured particle yields [3]. The red line marks the first order phase transition to nuclear matter. The dashed and dashed-dotted lines indicate an estimate for the range of applicability of our model. More specific, in the region to the right of the dashed line the relative contribution of pions to the pressure is smaller than 20%. In the region to the left of the dashed-dotted line the baryon density n_{Baryons} is smaller than 1.5 times the nuclear saturation density $n_{\text{nuclear}} = 0.153/\text{fm}^3$. In this region no signs of a phase transition are visible.

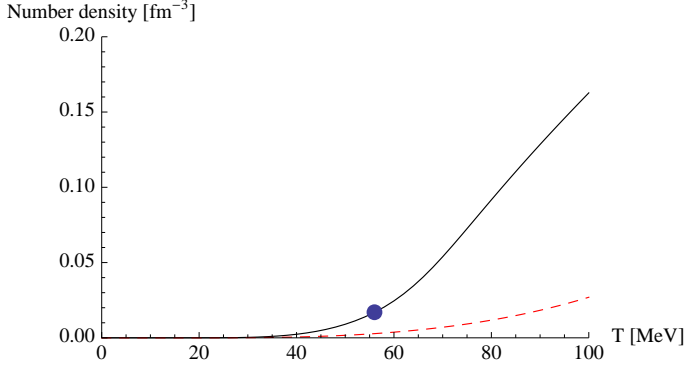


FIG. 2: Number density of baryons as a function of the temperature for $\mu = 750$ MeV (solid line). Note that the number of anti-baryons is negligible within the plot resolution. We also show the number of pions (dashed line). The dot marks the experimental result for the chemical freeze-out temperature $T_{\text{ch}} = 56^{+9.6}_{-2.0}$ MeV corresponding to $\mu_{\text{ch}} = 760 \pm 22.8$ MeV.

The computational task concerns then mainly the difference of the effective meson potential $U(\sigma; T, \mu) - U(\sigma; 0, \mu_c)$. This can be done by various methods – for example one could employ functional renormalization by adding nucleon degrees of freedom to the setting of ref. [10]. For our limited purpose a very simple approach will do. The potential difference is directly related to difference of pressure for the parameters $(\sigma; T, \mu)$ and $(\sigma; 0, \mu_c)$. This can be approximated by a free gas of nucleons with σ -dependent mass. We can consider σ as

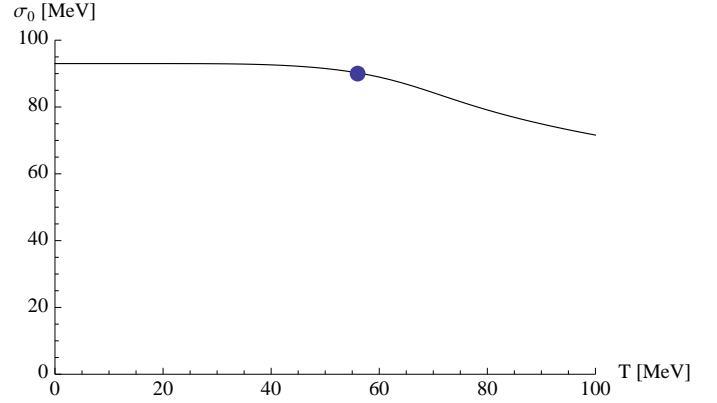


FIG. 3: Chiral order parameter as a function of the temperature for $\mu = 750$ MeV. The dot marks the experimental result for the chemical freeze-out temperature $T_{\text{ch}} = 56^{+9.6}_{-2.0}$ MeV corresponding to $\mu_{\text{ch}} = 760 \pm 22.8$ MeV.

an additional parameter in thermodynamics. Its value can be varied by varying the quark mass. If needed, meson fluctuations can be added in a similar way. We will discuss the linear nucleon-meson model in the setting of ref. [11]. (Our normalization of σ differs by a factor 2 from [11].) Our new results extend the analysis to non-vanishing temperature.

Linear nucleon-meson model

We use an effective model for baryons ψ_a (a is an isospin index with ψ_1 describing protons and ψ_2 neutrons), an isospin singlet vector meson ω_μ , a scalar meson σ and pseudo-scalar mesons $\pi^0 = \pi_3$, $\pi^\pm = \frac{1}{\sqrt{2}}(\pi_1 \pm i\pi_2)$. It is convenient to combine the scalars and pseudo-scalars in the field

$$\phi_{ab} = \begin{pmatrix} \frac{1}{\sqrt{2}}(\sigma + i\pi^0) & i\pi^- \\ i\pi^+ & \frac{1}{\sqrt{2}}(\sigma - i\pi^0) \end{pmatrix}. \quad (1)$$

The effective Lagrangian is of the form

$$\begin{aligned} \mathcal{L} = & \bar{\psi}_a i\gamma^\nu (\partial_\nu - ig\omega_\nu - i\mu\delta_{0\nu}) \psi_a \\ & + \sqrt{2}h [\bar{\psi}_a (\frac{1+\gamma_5}{2}) \phi_{ab} \psi_b + \bar{\psi}_a (\frac{1-\gamma_5}{2}) (\phi^\dagger)_{ab} \psi_b] \\ & + \frac{1}{2} \phi_{ab}^* (-\partial_\mu \partial^\mu) \phi_{ab} + U_{\text{mic}}(\rho, \sigma) \\ & + \frac{1}{4} (\partial_\mu \omega_\nu - \partial_\nu \omega_\mu) (\partial^\mu \omega^\nu - \partial^\nu \omega^\mu) + \frac{1}{2} m_\omega^2 \omega_\mu \omega^\mu. \end{aligned} \quad (2)$$

Here we use the chiral invariant scalar field combination $\rho = \frac{1}{2} \phi_{ab}^* \phi_{ab}$ and $U_{\text{mic}}(\rho, \sigma)$ is a microscopic form of the effective potential

$$U_{\text{mic}}(\rho, \sigma) = \bar{U}(\rho) - m_\pi^2 f_\pi \sigma. \quad (3)$$

The Lagrangian (2) is invariant under the chiral symmetry $SU(2)_V \times SU(2)_A \times U(1)_V \times U(1)_A$ where the nucleon

doublet transforms according to

$$\begin{aligned}\psi &\rightarrow \left(1 + \frac{i}{2}\alpha_V\boldsymbol{\tau} + \frac{i}{2}\alpha_A\boldsymbol{\tau}\gamma_5 + \frac{i}{2}\beta_V + \frac{i}{2}\beta_A\gamma_5\right)\psi, \\ \bar{\psi} &\rightarrow \bar{\psi}\left(1 - \frac{i}{2}\alpha_V\boldsymbol{\tau} + \frac{i}{2}\alpha_A\boldsymbol{\tau}\gamma_5 - \frac{i}{2}\beta_V + \frac{i}{2}\beta_A\gamma_5\right),\end{aligned}\quad (4)$$

where $\boldsymbol{\tau} = (\tau_1, \tau_2, \tau_3)$ are the Pauli matrices in isospin space and the scalar field transforms according to

$$\phi \rightarrow \phi - \frac{i}{2}\alpha_V[\boldsymbol{\tau}, \phi] - \frac{i}{2}\alpha_A\{\boldsymbol{\tau}, \phi\} + i\beta_A\phi. \quad (5)$$

The vector meson field ω_μ is invariant under the above symmetry. It couples to the conserved baryon number current associated with the $U(1)_V$ symmetry such that only the spin-one part of ω_μ plays a role while the spin-zero component $\partial_\mu\omega^\mu$ decouples.

The only explicit breaking of chiral symmetry comes from the quark masses. This is reflected by the linear term in the effective potential (3). Therefore U_{mic} depends explicitly on the field σ in addition to the invariant $\rho = \frac{1}{2}(\sigma^2 + \boldsymbol{\pi}^2)$. The scalar field σ will have a vacuum expectation value, in contrast to the pseudo-scalar field, $\pi^0 = \pi^+ = \pi^- = 0$. Due to rotational symmetry, only the zero-component of the vector field ω_μ can have an expectation value. Inspection of Eq. (2) shows that this can be interpreted as a shift in the effective chemical potential.

We are interested in the quantum effective potential $U(\sigma, \omega_0)$ which includes the effects of quantum and thermal fluctuations. It can be obtained from the quantum effective action - the generating functional for one-particle irreducible Greens functions - by specializing to constant σ and ω with $\psi = 0, \pi = 0$. The minimum of $U(\sigma, \omega_0)$ determines the expectation values for σ and ω_0 , i.e. the chiral order parameter and the effective chemical potential. In general, the computation of $U(\sigma, \omega_0)$ from a microscopic action is a complicated task. From the realization of symmetries we know, however, that the explicit symmetry breaking occurs only via the unaffected linear term,

$$U(\sigma, \omega_0) = U(\rho, \omega_0) - m_\pi^2 f_\pi \sigma, \quad \rho = \frac{1}{2}\sigma^2, \quad (6)$$

such that the task consists in a computation of the chirally invariant potential $U(\rho, \omega_0)$.

We are only interested in the difference $\Delta = U(\rho, \omega_0; T, \mu) - U(\rho, \omega_0; 0, \mu_c)$, with μ_c the value of the chemical potential at which the zero-temperature phase transition between a hadron gas and nuclear matter occurs. This simplifies our task considerably. Instead of a complicated computation of $U(\rho, \omega_0; 0, \mu_c)$ we can use observation in order to pin down the relevant properties of this quantity. In a functional renormalization approach the difference Δ involves only mesons with mass m smaller πT or baryons with $m - \mu_{\text{eff}}$ smaller than πT , where $\mu_{\text{eff}} = \mu + g\omega_0$ and ω_0 is the expectation value of ω_0 [10, 11]. In our range of interest these are essentially

nucleons and possibly pions, thus justifying the degrees of freedom incorporated in our model.

Furthermore, for the relatively narrow range in T and μ that we investigate here the running and the associated μ - and T -dependence of the couplings h and g is small and can be neglected. In a first approach we also neglect the subleading pion fluctuations. With these approximations the solution of functional flow equations actually reduces to performing a Gaussian functional integral over the fermionic fields ψ_N in a background of constant σ and ω_0 . This is nothing else than relativistic mean field theory. We stress that mean field theory is generically not expected to give reliable results in our setting with strong interactions. For example, a mean field computation of $U(\rho, \omega_0; 0, \mu_c)$ would fail badly. However, the more general view from a functional renormalization perspective permits to assess that the mean field result for Δ is reliable within an appropriate parameter range. We expect leading corrections from the omitted pion fluctuations. (They can be incorporated, in principle, in some type of extended mean field theory, see below.) To the right of the left dashed line in Fig. 1 the pion contributions to the pressure are less than 20 %. A second type of correction is expected due to the neglected σ -dependence of h, g and m_ω . In view of the small deviation of σ from its vacuum value visible in Fig. 3 we expect this effect to be small. It increases, however, for larger density and this is one of the restrictions for the limitation of validity of our model indicated by the right dashed line in Fig. 1.

We next discuss the mean field contribution to Δ which is directly related to the pressure of a free nucleon gas with field dependent masses. The corresponding contribution to the effective potential depends on the temperature T and chemical potential μ . It can be parametrized in terms of the pressure of a free gas of relativistic fermions and corresponding antiparticles

$$\begin{aligned}P_{\text{FG}}(T, \mu, m) &= \frac{1}{3} \int \frac{d^3p}{(2\pi)^3} \frac{\vec{p}^2}{\sqrt{\vec{p}^2 + m^2}} \\ &\times \left[\frac{1}{e^{\frac{1}{T}(\sqrt{\vec{p}^2 + m^2} - \mu)} + 1} + \frac{1}{e^{\frac{1}{T}(\sqrt{\vec{p}^2 + m^2} + \mu)} + 1} \right].\end{aligned}\quad (7)$$

Within our model, the effective potential for the bosonic fields reads now

$$U(\sigma, \omega_0; T, \mu) = U_{\text{vac}}(\sigma, \omega_0) - 4 P_{\text{FG}}(T, \mu + g\omega_0, h\sigma), \quad (8)$$

where the factor 4 accounts for the degeneracy in spin and isospin. For the effective potential in the vacuum (i. e. at $T = \mu = 0$) we use the parametrization

$$\begin{aligned}U_{\text{vac}}(\sigma, \omega_0) &= \frac{1}{2}m_\pi^2(2\rho - f_\pi^2) + \frac{1}{8}\lambda(2\rho - f_\pi^2)^2 \\ &+ \frac{1}{3}\frac{\gamma_3}{f_\pi^2}(2\rho - f_\pi^2)^3 + \frac{1}{4}\frac{\gamma_4}{f_\pi^4}(2\rho - f_\pi^2)^4 \\ &- m_\pi^2 f_\pi(\sigma - f_\pi) - \frac{1}{2}m_\omega^2\omega_0^2.\end{aligned}\quad (9)$$

For $T = 0$ the pressure $P_{FG}(0, \mu, m)$ vanishes identically for $\mu < m$. Thus Δ vanishes for $\mu < h\sigma - g\omega_0$ and the expressions in Eq. (8) and (9) coincide.

Parameters

At this point the open parameters of the model are

$$f_\pi, m_\pi, \lambda, \gamma_3, \gamma_4, m_\omega, h \text{ and } g. \quad (10)$$

We choose the experimentally established values $f_\pi = 93$ MeV for the pion decay constant, $m_\pi = 135$ MeV for the mass of pions and $m_\omega = 783$ MeV for the mass of the vector meson. The Yukawa coupling h is fixed by the requirement that hf_π equals the nucleon mass $m_n = 939$ MeV which gives $h = 10$. We have verified that somewhat smaller values of h (cf. ref. [11]) do not change our results qualitatively.

The remaining open parameters g, λ, γ_3 and γ_4 are fixed by requiring that the model describes at vanishing temperature $T = 0$ normal nuclear matter at the gas-liquid phase transition. More specific, the minimum of the effective potential (8) is at $\sigma = f_\pi$ for vanishing chemical potential μ and the baryon density $n_B = -\frac{\partial}{\partial \mu} U$ vanishes at this point. However, for increasing μ a second minimum at a smaller value of σ will develop and a first order phase transition takes place when the two minima are degenerate. From the nuclear binding energy $\epsilon_{\text{bind}} = -16.3$ MeV one can determine the critical chemical potential, $\mu_c = 939 \text{ MeV} - 16.3 \text{ MeV} = 922.7 \text{ MeV}$.

From minimizing the effective potential (8) with respect to ω_0 one finds the self-consistency equation

$$\omega_0 = -\frac{g}{m_\omega^2} n_B(0, \mu + g\omega_0, h\sigma) \quad (11)$$

with the baryon density

$$n_B(0, \mu + g\omega_0, h\sigma) = 4 \frac{\partial}{\partial \mu} P_{FG}(0, \mu + g\omega_0, h\sigma). \quad (12)$$

At μ_c the baryon density jumps from zero to nuclear saturation density $n_{\text{nucl}} = 0.153/\text{fm}^3$ this shows that also ω_0 changes discontinuously from $\omega_0 = 0$ to $\omega_{0,\text{nucl}}$ at the first order phase transition. From the Landau mass $m_L = \sqrt{h^2 \sigma_{\text{nucl}}^2 + p_F^2} = \mu_c + g\omega_{0,\text{nucl}}$ one can determine g and $\omega_{0,\text{nucl}}$. We use $m_L = 0.80 m_n$ for our numerical calculation, which gives $g = 9.5$ and $\omega_{0,\text{nucl}} = -18$ MeV. Using the relation $n_{\text{nucl}} = \frac{4}{6\pi^2} p_F^3$, one can also determine the position of the second minimum of the effective potential with respect to σ at the phase transition, $\sigma_{\text{nucl}} = 69.8$ MeV.

Of the remaining three parameters λ, γ_3 and γ_4 two get fixed by the constraints for a first order phase transition

$$U(\sigma_{\text{nucl}}, \omega_{0,\text{nucl}}; 0, \mu_c) = U(f_\pi, 0; 0, \mu_c) \quad (13)$$

and

$$\frac{\partial}{\partial \sigma} U(\sigma_{\text{nucl}}, \omega_{0,\text{nucl}}; 0, \mu_c) = 0. \quad (14)$$

The third parameter (say λ) can now be adapted to other properties of nuclear matter. For example, the choice $\lambda = 50, \gamma_3 = 3$ and $\gamma_4 = 50$ corresponds to the (vacuum) mass of the σ -meson $m_\sigma = \sqrt{\lambda f_\pi^2 + m_\pi^2} = 670$ MeV, the compressibility module $K = 9n/(dn/d\mu) = 300$ MeV and the surface tension of a nuclear droplet $\Sigma = \int_{\sigma_{\text{nucl}}}^{f_\pi} \sqrt{2U(\sigma)} d\sigma = 42000 \text{ MeV}^3$. Considered the simplicity of the model, these values are in reasonable agreement with the experimentally established values $m_\sigma \approx 484 \pm 17 \text{ MeV}$ [13], $K \approx 240 \pm 30 \text{ MeV}$ and $\Sigma \approx 42200 \text{ MeV}^3$.

As an independent check we determine for this choice of parameters also the “nuclear σ -term” which quantifies how the vacuum mass of the nucleon depends on the chiral symmetry breaking explicit mass term for the quarks. It can be determined by comparing the expectation value σ_{nuc} in the nuclear matter phase with the value obtained in the chiral limit, $m_\pi = 0$, for otherwise identical U_{vac} . One finds 40 MeV, in reasonable agreement with lattice calculations [14]. Overall, one finds a satisfactory agreement with nuclear matter at vanishing temperature and the nuclear droplet model. Our parameters are found in a similar range as the ones determined in ref. [11]. We have checked that other reasonable parameter choices do not modify our main conclusions.

Thermodynamic properties and chemical freeze-out

Let us now investigate the linear nucleon-meson model at non-zero temperature. We start from the effective potential $U(\sigma; T, \mu)$ which follows from Eq. (10) by minimizing with respect to the value of ω_0 . The complete information about the phase diagram and the thermodynamic properties is encoded in this quantity. For example, the chiral condensate $\sigma_0(T, \mu)$ is determined as the global minimum of $U(\sigma; T, \mu)$ with respect to σ . A phase transition of first order occurs when the potential has two local minima, such that at the critical temperature T_c the global minimum jumps discontinuously from one local minimum to the other. To illustrate this behavior we plot in Fig. 4 the effective potential $U(\sigma; T, \mu)$ as a function of σ for vanishing temperature $T = 0$ and different values of the chemical potential μ . One can clearly see the first order phase transition at the critical chemical potential $\mu_c = 922.7 \text{ MeV}$.

Let us now follow the changes in the effective potential as the temperature is increased. In Fig. 5 we plot $U(\sigma)$ for $\mu = \mu_c(T)$ and for different temperatures $T = 0$ ($\mu_c = 922.7 \text{ MeV}$), $T = 5 \text{ MeV}$ ($\mu_c = 921.3 \text{ MeV}$), $T = 10 \text{ MeV}$ ($\mu_c = 917.2 \text{ MeV}$), $T = 15 \text{ MeV}$ ($\mu_c = 910.8 \text{ MeV}$) and $T = 20 \text{ MeV}$ ($\mu_c = 902.3 \text{ MeV}$). One finds that the effective potential at the minima gets more negative as the temperature increases. This corresponds to an increase in pressure $p = -U_{\text{min}}$. One also finds that the potential barrier between the two minima becomes smaller, such that the surface tension for a droplet decreases. For $T_* = 20.7 \text{ MeV}$ and $\mu = 901 \text{ MeV}$ the barrier disappears

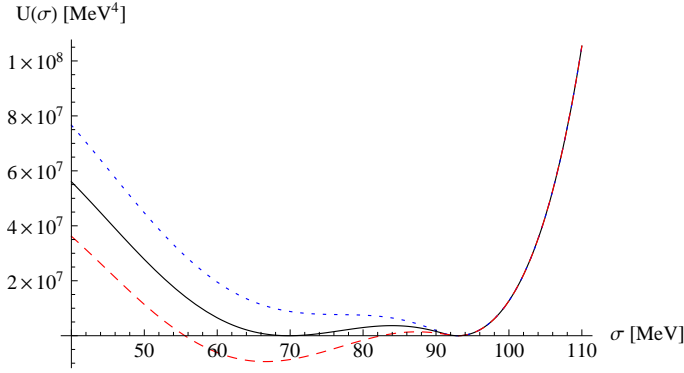


FIG. 4: Effective potential $U(\sigma)$ as a function of the chiral order parameter for $T = 0$ and chemical potential $\mu = 915$ MeV (dotted line), $\mu = 922.7$ MeV (solid line) and $\mu = 930$ MeV (dashed line).

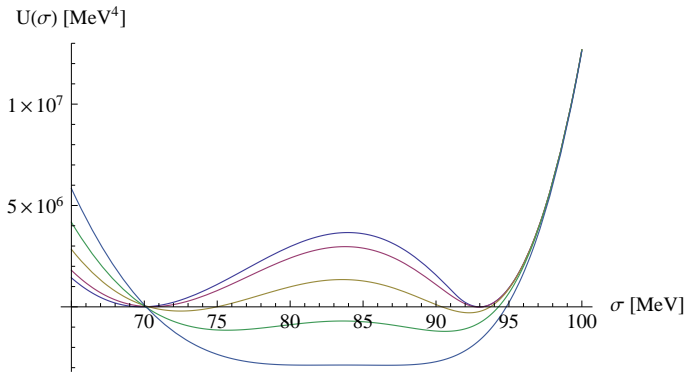


FIG. 5: Effective potential $U(\sigma)$ as a function of the chiral order parameter at the critical chemical potential of the first order phase transition $\mu = \mu_c(T)$ for temperatures $T = 0$, $T = 5$ MeV, $T = 10$ MeV, $T = 15$ MeV and $T = 20$ MeV.

and the line of first order phase transitions ends in a critical end point. The two minima merge into one. This is completely analogous to the critical endpoint for the water-vapor transition. The computed temperature for the endpoint, $T_* \approx 20$ MeV agrees well with observation, demonstrating the validity of our treatment of the linear nucleon-meson model.

Besides the first order gas-liquid phase transition, the effective potential (8) also exhibits another first order transition at larger values of the chemical potential. Here the chiral condensate jumps to much smaller values which vanish in the chiral limit $m_q = 0$. This transition could be associated with a transition from nuclear matter to quark matter and restoration of chiral symmetry. It is obvious that for quark matter the linear nucleon-meson model cannot give a valid description and we therefore cannot trust Eq. (8) in this region of the phase diagram. It is possible to modify the model in order to incorporate an effective change from nucleons to quarks. However, the existence and properties of a phase transition depend strongly on details of the change of effective degrees of

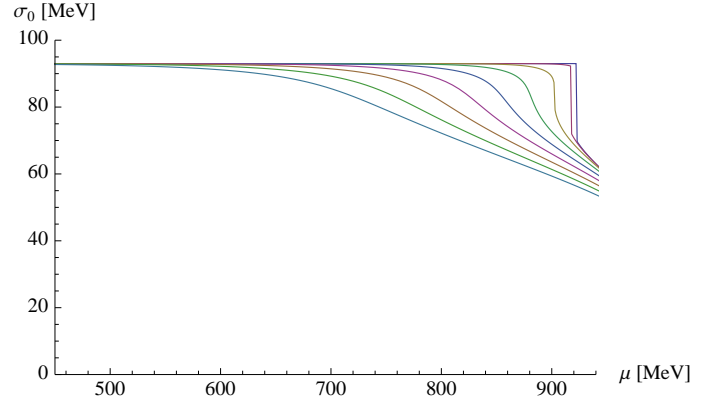


FIG. 6: Chiral order parameter σ_0 as a function of the chemical potential for $T = 0$ (uppermost curve), $T = 10$ MeV, $T = 20$ MeV, $T = 30$ MeV, $T = 40$ MeV, $T = 50$ MeV, $T = 60$ MeV, $T = 70$ MeV and $T = 80$ MeV (lowermost curve).

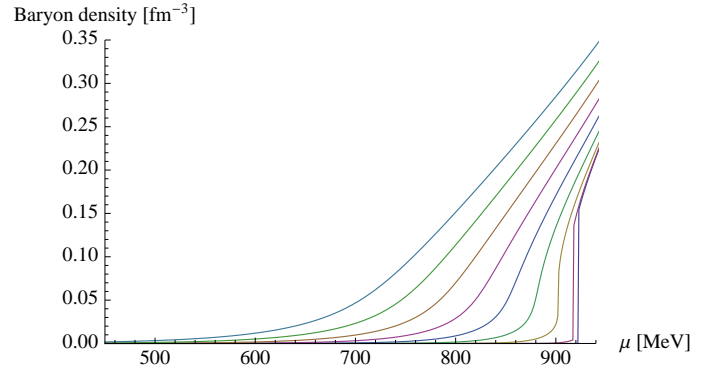


FIG. 7: Baryon number density as a function of the chemical potential for $T = 0$ (lowermost curve), $T = 10$ MeV, $T = 20$ MeV, $T = 30$ MeV, $T = 40$ MeV, $T = 50$ MeV, $T = 60$ MeV, $T = 70$ MeV and $T = 80$ MeV (uppermost curve).

freedom [11] such that no reliable information can be gained without a better understanding how nucleons are replaced by quarks. In practice, the chiral condensate in the vicinity of the gas-liquid transition is typically in the range $\sigma = 65 \dots 93$ MeV, while the additional minimum at larger chemical potential occurs at much smaller values, $\sigma < 10$ MeV. Obviously, the Taylor expansion of U_{vac} for σ around f_π in Eq. (9) is no longer reliable for such small values of σ . The investigations in ref. [11] show that the phase transition to quark matter (if it exists) occurs for baryon densities higher than the ones that would result from the linear nucleon-meson model. Our limitation to baryon densities smaller than 1.5 times nuclear density, as indicated in Fig. 1, is therefore a conservative estimate of the validity of our model.

For temperatures higher than the one of the critical endpoint $T_* = 20.7$ MeV one finds that the first order phase transition gets replaced by a crossover which gets rapidly rather smooth. To illustrate this we plot in Fig. 6

the chiral order parameter σ_0 as a function of the baryon chemical potential μ for various values of the temperature in the range $T = 0 \dots 80$ MeV. Similarly, Fig. 7 shows the baryon density n_B as a function of the chemical potential for the same temperatures. Together with Fig. 2 and Fig. 3 this demonstrates clearly that the observed chemical freeze-out points in the $\mu - T$ -diagram are far away from any phase transition or rapid crossover. This main result of the present letter contrasts with the properties of chemical freeze-out at low baryon density.

Still, the baryon density (or particle density if mesons are included) changes rapidly as a function of temperature in the range of interest, cf. fig. 2. The rates of processes with a change of particle numbers, as annihilation or production of strange particles, depends strongly on the number density of hadrons [4]. These processes stop effectively once the hadron density drops below a critical value. Since a rather small change of temperature corresponds to a substantial change in hadron density the chemical freeze-out occurs for a small temperature interval. This explains why common values of μ and T can describe rather well the abundancies of all hadron species. Even if the freeze-out number density for different hadrons differs to some extent, this will not have a large effect on the value of the freeze-out temperature.

We plot in Fig. 1 the line of constant baryon density, $n = 0.15 n_{\text{nuclear}}$. The observed freeze-out temperatures are well described by this line if the baryon density is high enough. We observe that any line with $n = c n_{\text{nuclear}}$, with $c < 1$, will end for low T in the line of the gas-liquid nuclear phase transition. This simply follows from the jump of n from $n = 0$ to $n = n_{\text{nuclear}}$ for $T = 0$. This explains why the observed freeze-out points tend to approach the first order nuclear phase transition. As we have seen, however, this should not be interpreted as a continuation of this first order line by a strong crossover.

We note as an aside that a freeze-out at constant baryon number density can explain also a puzzling feature of the chemical freeze-out volume per unit rapidity dV/dy . While this quantity grows with collision energy for the high energy experiments, the relation is reverse for $\sqrt{s_{NN}} \lesssim 4.5$ GeV [2]. However, assuming constant n_{Baryons} at freeze-out, the behavior at AGS energies reflects just the experimental finding for the energy dependence of the proton yield dN/dy at $y = 0$ [15].

In principle, a deviation of the chiral condensate σ_0 from its vacuum value f_π and a non-vanishing expectation value ω_0 (implying $\mu_{\text{eff}} = \mu + g\omega_0 \neq \mu$) should lead to modified particle yields with respect to a thermal model that assumes vacuum masses and $\mu = \mu_{\text{eff}}$. The chemical potential extracted from the thermal fits corresponds in first approximation actually to $\mu + g\omega_0 - h(\sigma_0 - f_\pi)$. However, we find the deviation of this quantity from μ to be small in the relevant regime, typically ~ 10 MeV.

We may also explore the phase diagram for temperatures higher than the freeze-out temperature. The temperature dependence of the number density and energy density for various values of μ is shown in figs. 8 and 9.

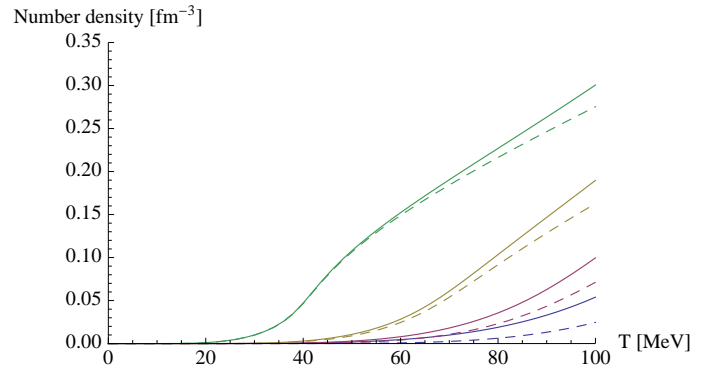


FIG. 8: Number density of baryons and pions (solid lines) as well as baryons only (dashed lines) as a function of temperature for the chemical potentials $\mu = 550$ MeV (lowermost curves), $\mu = 650$ MeV, $\mu = 750$ MeV and $\mu = 850$ MeV (uppermost curves).

Meson fluctuations

For our quantitative discussion we have not included the fluctuations of the π, σ , and ω mesons. We also did not consider their contribution to the particle density for hadrons. For an estimate of the validity of our approximation we may compute the contribution of the meson fluctuations to the effective potential, using a Gaussian approximation similar to the baryon fluctuations. For that purpose we assume that the momentum dependent parts of their inverse propagators are not modified by the effects of non-zero chemical potential and temperature, and we use a Gaussian or quasi-particle approximation. The effect of the bosonic fluctuations can then be parametrized in terms of the pressure of a free gas of relativistic bosons, $P_{\text{BG}}(T, \mu, m)$, completely analogous to Eq. (7). The masses of the pions and σ -mesons depend on σ according to

$$m_\pi^2(\sigma) = \frac{1}{\sigma} \left(\frac{\partial U}{\partial \sigma} + m_\pi^2 f_\pi \right), \quad m_\sigma^2(\sigma) = \frac{\partial^2 U}{\partial \sigma^2}, \quad (15)$$

while m_ω^2 is independent of σ in our approximation. Thus the ω -fluctuations contribute to U only a temperature dependent constant and we will neglect them. The Gaussian approximation becomes invalid in regions where $m_\pi^2(\sigma)$ or $m_\sigma^2(\sigma)$ become negative. Close to the value where $m_\pi^2(\sigma)$ vanishes it also matters if one evaluates $\partial U / \partial \sigma$ for the potential (8), as we do it here, or uses a self-consistent formulation where U includes the meson fluctuations. We stay away from such problematic regions.

The pion- and σ -contributions to the effective potential ΔU_m read

$$\Delta U_m = -3P_{\text{BG}}(T, 0, m_\pi(\sigma)) - P_{\text{BG}}(T, 0, m_\sigma(\sigma)). \quad (16)$$

Here P_{BG} obtains from Eq. (7) by setting $\mu = 0$, dropping the second term and replacing the fermionic by the

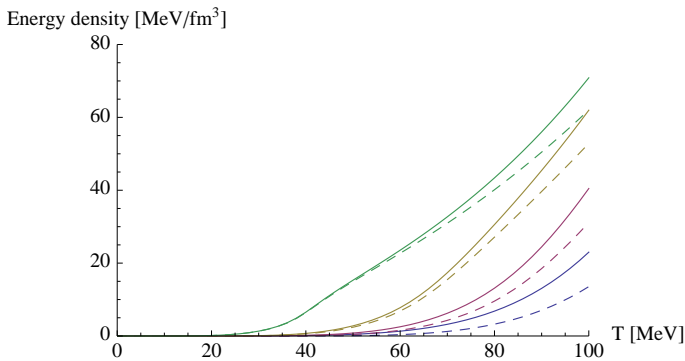


FIG. 9: Energy density of baryons and pions (solid lines) as well as baryons only (dashed lines) as a function of temperature for the chemical potentials $\mu = 550$ MeV (lowermost curves), $\mu = 650$ MeV, $\mu = 750$ MeV and $\mu = 850$ MeV (uppermost curves).

bosonic mean occupation number (changing +1 to -1 in the denominator). We have verified that the meson fluc-

tuations play only a minor role in the region of interest, as shown in Fig. 1 and 2. The relative importance of the pion fluctuations can be judged from figs. 8 and 9.

We conclude that the central result of this note seems to be rather robust. The chemical freeze-out at high baryon density is not related to any phase transition or rapid crossover. It rather follows a simple line of constant freeze-out density. We believe that the linear nucleon-meson model can give a reliable description for the whole low temperature region of the QCD-phase diagram up to densities of at least 1.5 times nuclear density. This requires the inclusion of the meson fluctuations, for example by a genuine functional renormalization group study.

Acknowledgment

S. F. acknowledges useful discussions with A. Andronic and financial support by DFG under contract FL 736/1-1.

-
- [1] P. Braun-Munzinger, J. Stachel, J. P. Wessels and N. Xu, Phys. Lett. B **344**, 43, (1995) and Phys. Lett. B **365**, 1, (1996); J. Cleymans, D. Elliott, H. Satz and R. L. Thews, Z. Phys. C **74**, 319 (1997); P. Braun-Munzinger, I. Heppe and J. Stachel, Phys. Lett. B **465**, 15 (1999); J. Cleymans, K. Redlich, Phys. Rev. C **60**, 054908 (1999); P. Braun-Munzinger, D. Magestro, K. Redlich and J. Stachel, Phys. Lett. B **518**, 41, (2001); F. Becattini, M. Gaździcki, J. Manninen, Phys. Rev. C **73**, 044905, (2006).
 - [2] A. Andronic, P. Braun-Munzinger and J. Stachel, Nucl. Phys. A **772**, 167 (2006).
 - [3] A. Andronic, P. Braun-Munzinger, J. Stachel, Phys. Lett. B **673**, 142 (2009); Erratum, Phys. Lett. B **678**, 516 (2009).
 - [4] P. Braun-Munzinger, J. Stachel and C. Wetterich, Phys. Lett. B, **596**, 61 (2004).
 - [5] Y. Aoki *et al.*, JHEP **0906**, 088 (2009).
 - [6] A. Bazavov *et al.*, e-print arXiv:1111.1710.
 - [7] A. Andronic *et al.*, Nucl. Phys. A **837**, 65 (2010).
 - [8] M. F. M. Lutz, B. Friman and C. Appel, Phys. Lett. B **474**, 7 (2000); N. Kaiser, S. Fritsch and W. Weise, Nucl. Phys. A **697**, 255 (2002); S. Fritsch, N. Kaiser and W. Weise, Phys. Lett. B **545**, 73 (2002); S. Fritsch, N. Kaiser and W. Weise, Nucl. Phys. A **750**, 259 (2005); for a recent overview see: W. Weise, Prog. Theor. Phys. Suppl. **186**, 390 (2010); e-print arXiv:1201.0950.
 - [9] J. D. Walecka, Ann. Phys. **83**, 491 (1974); see also: J. D. Walecka, *Theoretical Nuclear and Subnuclear Physics*, Second Edition, World Scientific, 2004.
 - [10] D. U. Jungnickel and C. Wetterich, Phys. Rev. **D53** (1996) 5142; In *Paris 1996, Quantum chromodynamics: Collisions, confinement and chaos* 139-175 [hep-ph/9610336]; In *Cambridge 1997, Confinement, duality, and nonperturbative aspects of QCD* 215-261 [hep-ph/9710397].
 - [11] J. Berges, D. U. Jungnickel and C. Wetterich, Int. J. Mod. Phys. A **18**, 3189 (2003) [hep-ph/9811387].
 - [12] J. -P. Blaizot, J. F. Berger, J. Dechargé and M. Girod, Nucl. Phys. A, **591**, 435 (1995)
 - [13] R. García-Martín, J. R. Peláez and F. J. Ynduráin, Phys. Rev. D **76**, 074034 (2007).
 - [14] S. Durr *et al.*, Phys. Rev. D **85**, 014509 (2012).
 - [15] J. L. Klay *et al.*, Phys. Rev. Lett. **88**, 102301 (2002).